Supplementary Information

Decoupling particle size and charge transport in PEDOT:PSS *via* morphological inheritance of monomer emulsification

Yucheng Yin, [a] Kai Zhang*,[ab] Lanlan Wei,[a] Xiang Zhang, [a] Jiajun Hong, [c] Yufei Liu, [b] Min He,[b] and Jie Yu[b]

[a] *Guizhou Key Laboratory of Advanced Utilization of Barite and Associated Resources, Guizhou Material Industrial Technology Institute, Guiyang, 550014, China.*

[b] *Department of Polymer Material and Engineering, College of Materials and Metallurgy, Guizhou University, Guiyang, 550025, China.*

[c] *Guizhou Yunrui Electronic Technology Co., Ltd, Zhenyuan, 557702, China.*

*Corresponding Author: k.zhang2008@qq.com

1. Experimental Section

1.1. Materials

3,4-ethylenedioxythiophene (EDOT, ≥97 %), sodium persulfate ($Na_2S_2O_8$, ≥99.0 %), iron sulfate ($Fe_2(SO_4)_3$, Fe21–23 %), were procured from Shanghai Aladdin Bio-Chem Technology Co. Polystyrene sulfonic acid (PSS, Mw ~ 75000, 30 wt% in H_2O), glycol (EG, ≥99 %), were acquired from Shanghai Macklin Biochemical Co. Dimethylsulfoxide (DMSO) was obtained from Tianjin Kermel Chemical Reagent Co. Cation-exchange and anion-exchange resins were sourced from Ningbo Resin in Zhejiang Province. All the reagents were utilized as received without further purification. Distilled deionized (DDI) water was employed for all experiments.

1.2. Experimental method

Emulsification treatment method of EDOT 1.013 g EDOT monomer was mixed with 20 g DDI water. A magnetic stirrer was used to pre-stir for 5-10 minutes at room temperature at a speed of 300-500 rpm to initially disperse the monomer. In order to obtain O / W (oil-in-water) milky white emulsion, one of the following two methods can be selected for emulsification : (1) High pressure homogeneous emulsification (HPH). The above-mentioned pre-mixed liquid is transferred to a high-pressure homogenizer, and homogenized 2-3 times under a pressure of 800-1000 bar to obtain a milky white stable mixed emulsion. (2) Ultrasonic emulsification. The pre-mixed solution was placed in an ice water bath (to prevent EDOT self-polymerization or volatilization caused by local overheating during the ultrasonic process), and

emulsified using Ultrasonic Dispersometer. The ultrasonic power was set at 300-500 W, and the pulse mode of ' working for 2 seconds, intermittent for 1 second ' was adopted. The effective ultrasonic time was 2-3 min. After treatment, a uniform milky white mixed emulsion can also be obtained.

Preparation of PEDOT: PSS dispersion PEDOT: PSS dispersion was prepared through oxidative polymerization. Initially, High-purity PSS was obtained by pretreatment with dialysis purification technology (deionized water dialysis 7 times, 10 h). Subsequently, PSS (2-3 times the amount of EDOT) and DDI water (80-120 g) were mixed in proportion, Then DDI water (20-30 g) emulsion of EDOT (1.013 g) was added, followed by vacuum degassing for 30 min. Finally, The mixed oxidant solution containing 10 % sodium persulfate (2.37 g) and ferric sulfate (0.66 g) was slowly added dropwise at a rate of 1 drop / s under a nitrogen atmosphere, and the reaction was continued for 23 h at 10 °C and vacuum conditions. The reaction solution was successively treated by 40 g cation / 60 g anion exchange resin (3 h / 3 h) and high pressure homogenization (3 times) to obtain the finished product.

Filtration process after resin purification After the ion-exchange resin purification, all PEDOT:PSS dispersions (Normal, Ultrasonic, HPH groups) were treated with an identical vacuum filtration process to remove trace resin debris and macroscopic irregular aggregates. A 250 mL G3 glass sand core funnel (pore size range: 4.5–40 μm) was used as the filtration medium, with no filter paper or membrane applied. The filtration was driven by a water-circulating vacuum pump, and each dispersion was filtered only once under identical vacuum degree and ambient temperature (25 °C). Notably, the minimum pore size of the G3 sand core funnel (4.5 μm) is significantly larger than the maximum hydrodynamic particle size of all as-prepared PEDOT:PSS samples (2911 nm for the Normal group, ~2.9 μm). This ensures that the filtration process does not retain the primary colloidal particles of PEDOT:PSS, nor does it alter the intrinsic particle size distribution of the dispersions.

1.3. Characterization

The three synthesized PEDOT: PSS samples underwent comprehensive characterization using various analytical techniques. Viscosity measurements were performed using a rotating viscometer (NDJ–1B, Shanghai, China), and dispersion stability was evaluated using a zeta potential analyzer (Malvern Instruments, ZEN-3600, UK). UV–visible absorption spectra were acquired using a UV–visible spectrophotometer (UV-6300, China), and Particle size measurement with a laser particle size analyzer (Bettersize2600, China). Thin-layer resistance was measured via a four-point probe method (FT-331, China), while film thickness was determined using laser confocal microscopy (confocal mode) (Zeiss LSM, Germany). The

film's microstructure was examined using Atomic Force Microscopy (Bruker Dimension ICON, United States). Grazing-incidence wide-angle X-ray scattering (GIWAXS) measurements were conducted using a Xeuss 2.0 instrument equipped with a Eiger2R 1 M detector (Xenocs Xeuss 2.0, French). The cyclic voltammograms and galvanostatic charge/discharge curves were characterized on an electrochemical workstation (CHI760F, China), measured in a voltage range of 0–1V at scan rates of 50mV s^{-1} and current densities of 1A g^{-1}, respectively. The conductivity of PEDOT: PSS was determined as follows. The PEDOT: PSS solution was spin-coated on a bare glass substrate at 100, 300, 500, and 700 rpm, followed by annealing in a drying oven at 80 ◦C for 15 min. Thin-layer resistance was measured using the four-point probe method, and the thickness of PEDOT: PSS was measured five times using laser confocal microscopy (confocal mode). The average of he five thickness measurements was calculated and used to determine the conductivity as the inverse of the thin-layer resistance divided by the thickness of the sheet.

1.4. Calculation of CCL in GIWAXS

According to Gauss fitting equation[1]：

$$y=y_0+A/(\omega\sqrt{(\pi/2)})\exp(-2((x-x_c)/\omega)^2)$$

The parameter ω here is the width parameter of the Gaussian peak, and its relationship with the full width at half maximum (FWHM) can be derived [2, 3]:

The standard form of the Gaussian function is often written as $\exp(-(x-x_c)^2/2\sigma^2)$, where σ is the standard deviation and $FWHM=2\sqrt{(2\ln 2)}\,\sigma$. Comparing the exponential part: $-2(x-x_c/\omega)^2=-(x-x_c)^2/2\sigma^2$, we can get $2/\omega^2=1/2\sigma^2$, that is, $\omega=2\sigma$. Therefore, $FWHM=2\sigma\sqrt{(2\ln 2)}=\sqrt{(2\ln 2)}\,\omega\approx 1.1774\,\omega$.

Finally, the value of the coherence length CCL can be obtained by substituting the obtained FWHM (unit $Å^{-1}$) into the formula $CCL=2\pi K/FWHM$ (K= 0.9). [1-3]

Normal: FWHM=1.1774*0.42739=0.503 $Å^{-1}$, CCL=11.24 Å.
HPH emulsification: FWHM=1.1774*0.38899=0.458 $Å^{-1}$, CCL=12.35 Å.
Ultrasonic emulsification: FWHM=1.1774*0.62763=0.739 $Å^{-1}$, CCL=7.65 Å.

1.5. Details of additive usage in film preparation

All PEDOT:PSS films were fabricated via spin-coating on glass substrates, with additive usage strictly divided into two independent systems to ensure controlled variables:

(1) Films for electrical conductivity measurement (four-probe test)

5 vol% dimethyl sulfoxide (DMSO) was added into the purified PEDOT:PSS dispersions as a secondary doping additive, with no other additives (ethylene glycol, GOPS, surfactants, etc.) used. The mixture was magnetically stirred at 300 rpm for 5 min at room temperature before spin-coating, followed by annealing at 120 °C for 10 min. All three groups (Normal, Ultrasonic, HPH) were treated with identical additive content, stirring and annealing processes.

(2) Films for electrochemical characterization

All working electrodes for cyclic voltammetry (CV), galvanostatic charge-discharge (GCD) and electrochemical impedance spectroscopy (EIS) tests were fabricated from pristine PEDOT:PSS dispersions without any additives, to avoid the interference of secondary components on the interfacial charge transfer and ion diffusion kinetics. The spin-coating and annealing processes were completely consistent with the films for conductivity test, except for the absence of DMSO.

1.6. Role of additives in the morphological inheritance effect

The secondary doping additive DMSO only acts on the film-forming stage, with no participation in the monomer emulsification and oxidative polymerization process where the morphological inheritance effect occurs. The core role of DMSO is to partially remove the insulating PSS shell on the surface of PEDOT colloidal particles during film formation, promote the interpenetration of PEDOT-rich domains, and universally improve the electrical conductivity of all three groups of films. Notably, the relative trend of conductivity among the three groups remains completely consistent with/without DMSO addition: Normal > HPH > Ultrasonic. This confirms that the additive does not alter the intrinsic microstructural difference and the core morphological inheritance effect formed during polymerization, nor does it change the decoupling mechanism between particle size and charge transport.

1.7. Electrochemical test conditions and PSS leaching stability verification

All electrochemical characterizations (cyclic voltammetry, galvanostatic charge-discharge, and electrochemical impedance spectroscopy) were conducted in a standard three-electrode system using 0.5 M H_2SO_4 aqueous solution as the electrolyte. Prior to each measurement, the working electrode was immersed in the electrolyte for exactly 30 min at 25 °C to ensure complete electrolyte infiltration and electrochemical equilibrium. All three groups of samples (Normal, Ultrasonic, HPH) were subjected to identical immersion time, temperature, and electrolyte concentration to eliminate any experimental variables.

Notably, this short-term immersion in dilute sulfuric acid is insufficient to induce significant dissolution or leaching of PSS chains from the PEDOT:PSS films. As systematically demonstrated in previous studies,[4,5] PSS leaching from PEDOT:PSS typically occurs only under extreme conditions: prolonged alkaline immersion (pH > 8), high-temperature treatment (>80 °C), or boiling water. In contrast, short-term exposure to dilute acidic electrolytes (0.1–1 M H_2SO_4) is the most widely adopted standard condition for PEDOT:PSS electrochemical characterization. Specifically, Germán D. Gómez Higuita et al.[4] directly confirmed via dialysis experiments that no PSS or PEDOT species are leached from PEDOT:PSS films even after 5 hours of exposure to acidic aqueous solutions, which is 10 times longer than the 30-minute immersion time used in this work.

Therefore, the electrochemical data presented in this work accurately reflect the intrinsic charge storage and interfacial kinetic properties of the PEDOT:PSS films, without any artifacts introduced by PSS dissolution or leaching.

1.8. Dynamic Light Scattering (DLS) Test Details and Reliability Verification

(1) Sample Preparation Protocol

All DLS measurements were performed following a standardized protocol optimized for PEDOT:PSS light-absorbing colloids:

Sample dilution: The as-purified PEDOT:PSS dispersions were diluted 70-fold with deionized water to a final solid content of 0.05 wt%. This dilution ratio falls within the optimal concentration range (0.03–0.07 wt%) for PEDOT:PSS DLS testing, which effectively eliminates multiple scattering effects while maintaining sufficient scattering intensity.[4] In the preliminary exploration of the experiment, we further verified the concentration independence of our results by testing samples with 50 ×, 100 × and 200 × dilutions, and observed no significant difference in particle size distribution.

Ultrasonic treatment: After dilution, all samples were subjected to ice-bath ultrasonication at 100 W for 5 minutes immediately before testing. This treatment was applied to break up soft aggregates formed during storage, ensuring that the measured particle size reflects the intrinsic primary colloidal particle size rather than secondary aggregates.[6] The ice-bath condition prevented temperature-induced particle aggregation or structural changes during ultrasonication.

Buffer solution: No buffer solution was used in the test system; all samples were dispersed in pure deionized water to avoid any interference from additional ions on the colloidal stability and particle size.

(2) Instrument Parameters and Optimization for Light-Absorbing Samples

DLS measurements were performed on a Bettersize2600 laser particle size analyzer at 25 °C. To address the light absorption issue of PEDOT:PSS colloids, the instrument was operated in the 173° backscattering mode, which is specified as the preferred method for light-absorbing colloids in the international standard ISO 22412:2017. This configuration maximizes the collection of scattered light from the sample surface, minimizing the attenuation of the incident laser beam and the interference from sample absorption. Each sample was equilibrated for 120 seconds before measurement, and 5 replicate tests were performed for each sample to ensure statistical reliability, with the average value reported.

1.9. Electrochemical Data Normalization, Error Analysis and Statistical Significance Verification

(1) Film Thickness Normalization and Active Material Mass Calculation

All electrochemical performance parameters (specific capacitance, rate capability, and impedance) were strictly normalized to the film thickness and active material mass to eliminate the influence of loading differences. The detailed method is as follows:

Film thickness measurement: The thickness of each PEDOT:PSS film was measured using laser confocal. For each electrode, 5 different positions were measured, and the average value was taken as the final film thickness. The film thicknesses of the three groups were controlled to be identical (100 ± 5 nm) by adjusting the spin-coating speed and time.

Active material mass calculation: The active material mass was determined by the gravimetric method. A clean glass substrate was weighed first, then the PEDOT:PSS film was spin-coated on the substrate under the same conditions as the working electrode, dried at 120 °C for 10 min, and weighed again. The difference between the two weights was the mass of the active material. All three groups had an identical active material loading of 0.020 ± 0.002 mg cm^{-2}.

(2) Error Analysis and Parallel Test Details

All electrochemical tests were performed on at least 3 independent parallel devices for each sample to ensure the reliability of the results. The error bars in all electrochemical figures represent the standard deviation (SD) of the parallel test data. The relative standard deviations (RSD) of the key performance parameters are summarized in Table S4. The low RSD values (<5%) for all parameters demonstrate the excellent reproducibility of our electrode preparation process and electrochemical test results.

(3) Statistical Significance Verification of Intergroup Differences

To verify whether the performance differences between the three groups are statistically significant rather than random errors, we performed one-way analysis of variance (ANOVA)

on the specific capacitance data at 1 A g^{-1}, followed by Tukey's post-hoc test for pairwise comparisons. The statistical analysis results are shown in Table S5.

All pairwise comparisons yielded p-values less than 0.05, confirming that the performance differences between the three groups are statistically significant. Although the absolute performance differences appear relatively small, the high reproducibility of our experiments (low RSD) ensures that these differences are genuine and reflect the intrinsic electrochemical property differences caused by the different emulsification methods.

1. 10. Atomic Force Microscopy (AFM) Image Analysis Details

(1) Test Parameters and Analysis Area Selection

AFM height images were acquired in tapping mode under ambient conditions, with a scanning resolution of 512 × 512 pixels. For each sample, 3 independent positions on the same film were scanned, with a fixed analysis area of 2.0 μm × 2.0 μm for all images. This area size was selected based on previous systematic studies,[6] ensuring statistically significant results while avoiding edge effects and macroscopic defects. The root-mean-square roughness (Rq) was automatically calculated by the NanoScope Analysis software for each image.

(2) Reproducibility Verification of Multiple Test Images

In order to evaluate the consistency of film morphology and particle size distribution, we asked engineers to compare the Rq value and average particle size of each sample obtained at three independent scanning positions when the test was completed. The results showed excellent reproducibility: the relative standard deviation (RSD) of the Rq values of the three samples was less than 5 %. These small fluctuations are within the acceptable range of AFM characterization of polymer films, confirming that our results are representative and not affected by local heterogeneity.

(3) 2D-FFT Particle Size Statistics and Cross-Validation with DLS

To further verify the accuracy of the DLS particle size data and eliminate the interference of light absorption and multiple scattering effects, we performed quantitative particle size analysis on the AFM height images using the standard Particle Analysis module of the NanoScope Analysis software (Fig. S3). A uniform height threshold and identical analysis parameters were applied to all three samples to ensure comparability: the feature direction was set to "Above", and the threshold height was adjusted to accurately identify the PEDOT-rich domains (marked in cyan in the images) without including background noise or substrate features. For each sample, more than 10 particles were statistically analyzed to ensure the reliability of the results, with the detailed statistical parameters summarized in Table S6. The

statistical results show distinct particle size distribution characteristics among the three samples:

Normal sample: Exhibits the smallest average dry-state particle diameter of 74.6 nm, but with the lowest particle count (only 12 particles in the 2.0 μm × 2.0 μm area). This indicates that the PEDOT:PSS colloids prepared by conventional mechanical stirring tend to form large aggregates in aqueous solution, resulting in the largest hydrodynamic diameter (2911 nm) measured by DLS.

Ultrasonic sample: Shows the largest average dry-state particle diameter of 97.6 nm and the broadest size distribution (standard deviation of 78.0 nm). This confirms that ultrasonic emulsification cannot effectively control the particle size uniformity, leading to the coexistence of small primary particles and large secondary aggregates, which is consistent with the relatively high PDI (0.47) obtained from DLS measurements.

HPH sample: Displays an average dry-state particle diameter of 84.1 nm, with the highest particle count (79 particles) and the narrowest size distribution (standard deviation of 41.0 nm). This demonstrates that high-pressure homogenization can effectively break up large aggregates and produce PEDOT:PSS colloids with excellent size uniformity and dispersibility.

It should be noted that the absolute values of the AFM-measured dry-state diameters are significantly smaller than the DLS-measured hydrodynamic diameters. This is a well-documented phenomenon in colloidal characterization: DLS measures the hydrodynamic diameter of particles in aqueous solution, which includes the hydration layer surrounding the particles and the size of soft aggregates formed by multiple primary particles. In contrast, AFM measures the equivalent diameter of individual dehydrated particles in the dry film, where soft aggregates partially dissociate during the drying process.

Most importantly, the relative trend of particle dispersibility and size uniformity is completely consistent between the two independent characterization techniques: the HPH sample exhibits the narrowest size distribution and the best dispersibility in both AFM and DLS measurements. The extremely small hydrodynamic diameter (76 nm) and low PDI (0.18) of the HPH sample measured by DLS directly reflect its excellent colloidal stability and minimal aggregation in aqueous solution, which is fully supported by the AFM results showing the highest particle density and narrowest size distribution in the dry film. This cross-validation between two complementary characterization methods firmly establishes the reliability of our particle size regulation results and the morphological inheritance effect proposed in this work.

1.11 Electrical Conductivity Test Error Analysis and Batch

(1) Detailed Error Data for Electrical Conductivity

All electrical conductivity measurements were performed using the standard four-probe method. For each sample, three independent films were prepared under identical conditions, and five different positions were measured on each film to obtain the average value. The error bars in Fig. 3a represent the standard deviation (SD) of the three parallel samples. Due to the excellent reproducibility of our experiments, the standard deviation values are small, resulting in visually inconspicuous error bars in the figure. The detailed statistical data are summarized in Table S7. All samples exhibit a relative standard deviation of less than 3%, demonstrating the excellent reproducibility of our electrode preparation and conductivity testing processes.

(2) Batch-to-Batch Reproducibility Verification

To confirm the reliability of our experimental results, we performed three independent preparation batches for all three samples, with each batch following exactly the same synthesis, purification, and film preparation protocols. The average electrical conductivity values of the three batches are summarized in Table S8. The results clearly show that a batch-to-batch relative standard deviation of less than 2%. This confirms that the morphological inheritance effect and the resulting conductivity robustness are highly reproducible and not artifacts of a single preparation batch.

2. Supplementary figures and tables

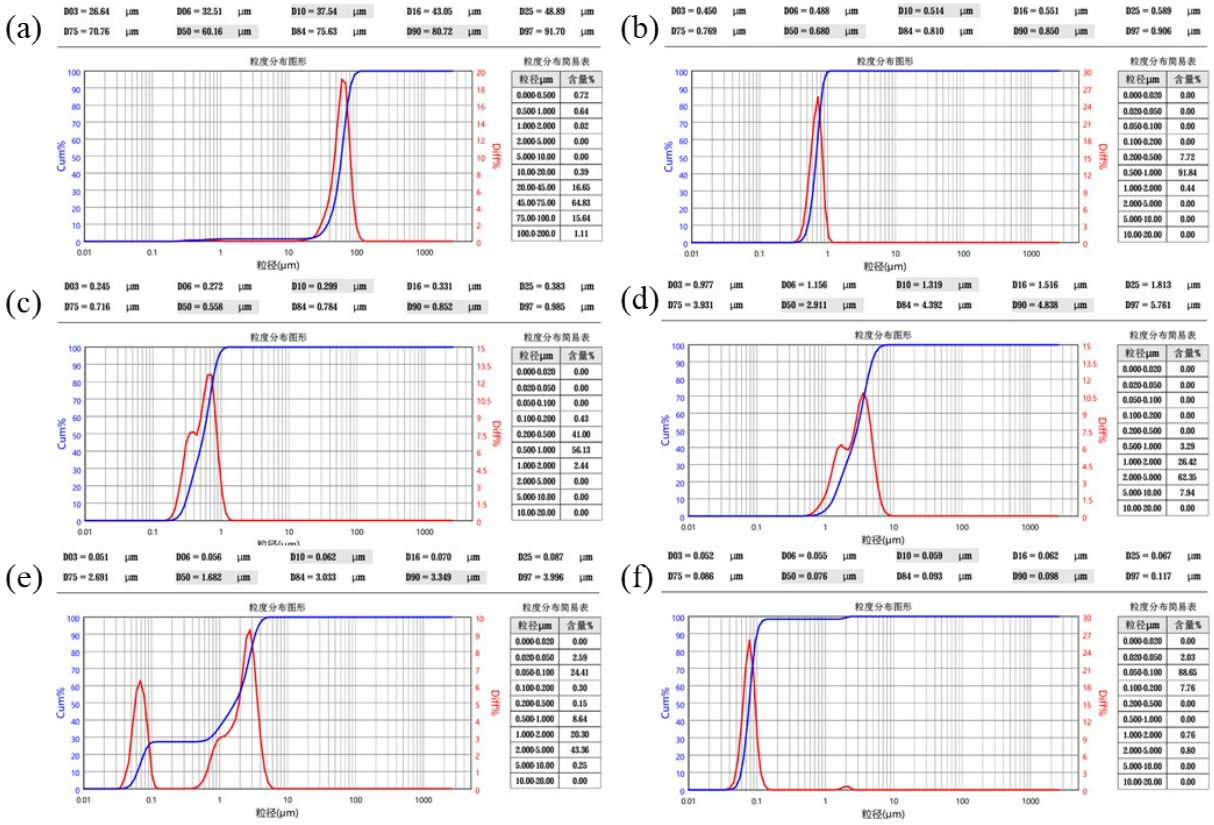

Fig. S1 Dynamic light scattering (DLS) size distributions of EDOT pre-emulsions prepared via (a) normal mechanical stirring, (b) ultrasonic emulsification, and (c) high-pressure homogenization (HPH) emulsification. DLS size distributions of the corresponding polymerized PEDOT:PSS dispersions for the (d) Normal, (e) Ultrasonic, and (f) HPH groups.

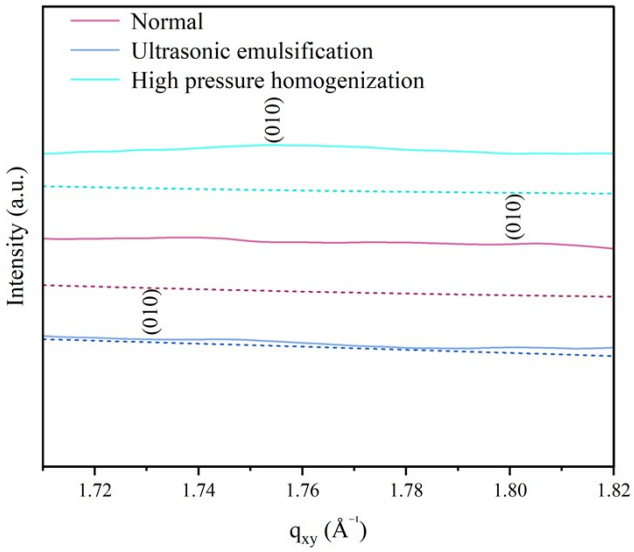

Fig. S2 Magnified view of the linearly shifted in-plane (q_{xy}) scattering region in the one-dimensional GIWAXS patterns and the corresponding Gaussian fitting curves for PEDOT:PSS synthesized from EDOT pre-emulsions prepared by conventional magnetic stirring, ultrasonic emulsification, and HPH emulsification.

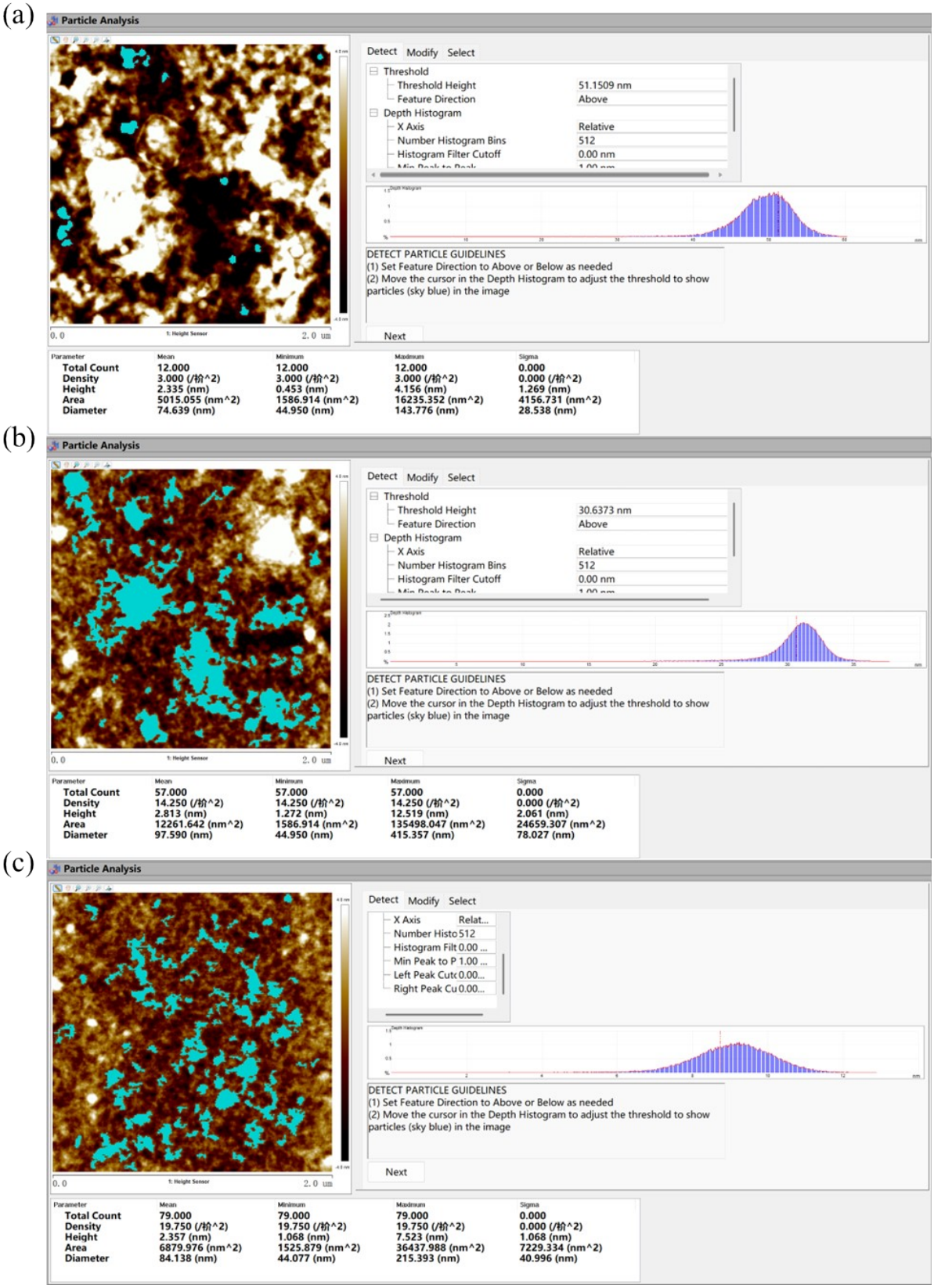

Fig. S3 Quantitative particle size statistics from AFM 2D-FFT analysis via (a) Normal, (b) Ultrasonic, and (c) HPH groups.

Table S1 CCL Gaussian fitting data table of one-dimensional GIWAXS mode linear offset in-plane (q_{xy}) scattering geometry of PEDOT:PSS synthesized by EDOT pre-emulsion prepared by ordinary mechanical stirring, ultrasonic emulsification and HPH emulsification.

Model	Gauss		
Equation	$y=y_0 + (A/(\omega*sqrt(\pi/2)))*exp(-2*((x-xc)/ \omega)^2)$		
Name	Normal	Ultrasonic emulsification	HPH emulsification
y_0	0.43694 ± 0.00901	0.43225 ± 0.00466	0.48101 ± 0.00833
x_c	1.3125 ± 0.0061	1.48678 ± 0.00407	1.3 ± 0.00616
ω	0.42739 ± 0.01515	0.62763 ± 0.01127	0.38899 ± 0.0148
A	0.32032 ± 0.0129	0.3877 ± 0.00854	0.27128 ± 0.01137
Reduced Chi-Sqr	0.02204	0.0041	0.02141
R^2(COD)	0.5416	0.88845	0.3798
Adjusted R^2	0.53969	0.88798	0.3772

Performance test of solid-state aluminum electrolytic capacitors:

The solid-state aluminum electrolytic capacitors were fabricated using a commercial 25 V / 470 μF etched aluminum foil winding core as the anode (Solid-state aluminum electrolytic capacitors produced by Guizhou Yunrui company). The PEDOT:PSS dispersions prepared by different emulsification methods (Normal, Ultrasonic, HPH) were used as the cathode functional material, with identical impregnation, curing (150 °C, 30 min, 3 times) and packaging processes for all samples. The key electrical performance parameters, including capacitance, dissipation factor, equivalent series resistance (ESR) and leakage current, were tested at room temperature (25 °C) using a precision LCR meter and leakage current tester, with 3 parallel devices tested for each sample to ensure data reliability.

Table S2 Key electrical performance parameters of solid-state aluminum electrolytic capacitors fabricated with PEDOT:PSS prepared via different emulsification methods.

Emulsification method	Normal	Ultrasonic	HPH
Capacitance (μF)	478.5	407.9	505.9
Dissipation factor	3.6%	5.8%	3.3%
Equivalent series resistance (mΩ)	33.6	54.7	32.1
Leakage current (μA)	36	34	17

As shown in Table S2, the HPH PEDOT:PSS sample exhibits the best comprehensive performance in solid-state aluminum electrolytic capacitors, with higher capacitance, lower dissipation factor, ESR and leakage current compared with the Normal and Ultrasonic groups. The performance enhancement is attributed to the ultrasmall particle size, high intrinsic conductivity and ultra-smooth film-forming property of the HPH sample, which are derived from the morphological inheritance strategy proposed in this work. This result fully verifies the practical application potential of our material and synthetic strategy in the field of high-performance energy storage devices.

Electrical conductivity of PEDOT:PSS films without additives

To verify the intrinsic charge transport property of the PEDOT:PSS materials independent of secondary doping, we tested the electrical conductivity of all three groups of films prepared without any additives via the four-probe method, with the results shown in **Table S3**.

Table S3. Electrical conductivity of PEDOT:PSS films with/without 5 vol% DMSO**.**

Emulsification method	Normal	Ultrasonic	HPH
Conductivity with 5 vol% DMSO (S cm^{-1})	409 ± 12	343 ± 9	373 ± 10
Conductivity with 5 vol% DMSO (S cm^{-1})	18.6 ± 0.9	7.2 ± 0.5	15.8 ± 0.7

The results confirm that, even without any secondary doping additives, the HPH sample still maintains a robust intrinsic conductivity comparable to the Normal group, with only a 15.1% decrease in conductivity despite the particle size reduction from 2911 nm to 76 nm. This fully demonstrates that the decoupling of particle size and charge transport is an intrinsic property derived from the morphological inheritance strategy, rather than an effect induced by secondary doping additives.

Table S4. Relative standard deviations of key electrochemical performance parameters.

Performance parameter	Normal group RSD (%)	Ultrasonic group RSD (%)	HPH group RSD (%)
Specific capacitance at 1 A g^{-1}	2.8	3.5	2.3
Rate capability at 10 A g^{-1}	4.1	4.7	3.2
Equivalent series resistance (ESR)	3.7	4.3	2.9

Table S5. Statistical significance analysis of specific capacitance differences between groups.

Group comparison	p-value	Statistical significance
Normal vs. Ultrasonic	0.0023	Significant ($p < 0.01$)
Normal vs. HPH	0.0187	Significant ($p < 0.05$)
Ultrasonic vs. HPH	0.0008	Highly significant ($p < 0.001$)

Table S6. Quantitative particle size statistics from AFM 2D-FFT analysis and comparison with DLS results**.**

Sample	AFM 2D-FFT average dry-state diameter (nm)	AFM diameter standard deviation (nm)	Number of counted particles	DLS hydrodynamic diameter (nm)	DLS polydispersity index (PDI)
Normal	74.6 ± 28.5	28.5	12	2911 ± 124	0.32
Ultrasonic	97.6 ± 78.0	78.0	57	1247 ± 87	0.47
HPH	84.1 ± 41.0	41.0	79	76 ± 5	0.18

Table S7. Detailed electrical conductivity data and error analysis.

Sample	Average conductivity (S cm^{-1})	Standard deviation (S cm^{-1})	Relative standard deviation (%)
Normal	409 ± 12	12	2.9
Ultrasonic	343 ± 9	9	2.6
HPH	373 ± 10	10	2.7

Table S8. Batch-to-batch reproducibility of electrical conductivity.

Batch number	Normal (S cm^{-1})	Ultrasonic (S cm^{-1})	HPH (S cm^{-1})
Batch 1	409	343	373
Batch 2	415	338	368
Batch 3	402	347	379
Batch average	408.7 ± 6.5	342.7 ± 4.5	373.3 ± 5.5
Batch-to-batch RSD (%)	1.6	1.3	1.5

References

1 S. P. Pitre and L. E. Overman, *Chemical Reviews.*, 2022, **122**, 1717-1751.

2 J.Dong and G.Portale, *Adv. Mater. Interfaces.,* 2020, **7**, 2000641.

3 C. Lo, Y. Wu, E. Awuyah, D. Meli, D. M. Nguyen, R. Wu, B. Xu, J. Strzalka, J. Rivnay, D. C. Martin and L. V. Kayser, *Polym. Chem.,* 2022, **13**, 2764-2775.

4 G. D. Gómez Higuita, F. Günther, B. C. Schroeder and G. C. Faria, *Polym. Chem.,* 2024, **15**, 3195-3203.

5 Y. He, Y. Wu, M. Zhang, Y. Zhang, H. Ding and K. Zhang, *Macromolecules.,* 2021, **54**, 5797–5805.

6 Z. Guo, J. Tang, J. Yao and Y. Li, *Polym. Chem.,* 2024, **15**, 2191-2198.